East European Journal of Physics. **4.** 318-325 (2023)
DOI:10.26565/2312-4334-2023-4-42 ISSN 2312-4334

SIMULTANEOUS DOCKING OF ANTIVIRAL DRUGS AND CYANINE DYES WITH PROTEINS USING MULTIPLE LIGAND APPROACH

Olga Zhytniakivska*, Uliana Tarabara, Kateryna Vus, Valeriya Trusova, Galyna Gorbenko
Department of Medical Physics and Biomedical Nanotechnologies, V.N. Karazin Kharkiv National University
4 Svobody Sq., Kharkiv, 61022, Ukraine
**Corresponding Author: olga.zhytniakivska@karazin.ua*
Received October 7, 2023; revised November 10, 2023; accepted November 17, 2023

The protein-based nanosystems for targeted drug delivery of a wide array of substances, ranging from small drugs and therapeutic proteins to nucleic acids and genes, attract increasing attention due to their biocompatibility and biodegradability, extraordinary binding capacity for different ligands, accessibility from natural sources, effective drug protection and gentle encapsulation conditions. Due to the multitude of binding pockets and functional groups on the protein surface, these nanocarriers seem to be highly efficient multifunctional nanotheranostic systems that could incorporate both a therapeutic drug and a visualizing agent. This integration serves multiple purposes, including the regulation of drug release, monitoring the alterations at the target site in response to treatment, and offering crucial insights into the efficacy of the intervention in its early stages. The development of these advanced nanosystems necessitates a thorough comprehension of the potential interactions within these intricate systems. In the present study we assessed the potential of six trimethine and seven pentamethine cyanine dyes to serve as visualizing agents in the drug-protein-dye systems which include functionally significant proteins (cytochrome *c*, serum albumin, lysozyme and insulin and four antiviral drugs, *viz.* favipiravir, molnupiravir, nirmatrelvir and ritonavir. The ternary systems with the highest dye-protein surface shape complementarity were established for all groups of the examined cyanine dyes. The influence of the cyanine dye structure on the stability of the drug-protein-dye complexes was assessed. The obtained results indicate that the dye-protein affinity is not solely dependent on the length of the polymethine chain. It was found that the most prospective drug delivery systems containing the trimethines and pentamethines as visualizing agents are AK5-6-, AK5-8- and AK3-11-drug-albumin complexes.
Keywords: *Protein-drug-dye complexes, Antiviral agents, Protein nanoparticles, Drug nanocarriers, Cyanine dyes, Multiple molecular docking*
PACS: 87.14.C++c, 87.16.Dg

During the past decades the field of engineering materials for drug delivery applications in cancer therapy [1-3], central nervous system indications [4,5], antiviral therapy [6,7], inflammatory [8,9] and cardiovascular diseases [10,11] has witnessed a growing interest in utilizing the nanostructured drug delivery systems (DDS). The evolution of these second-generation DDSs offers a range of advantages that aim to tackle numerous challenges associated with conventional therapies including: i) enhanced stability and solubility of drugs; ii) reduced drug toxicity; iii) uniform dosing; iv) improved drug pharmacokinetics and distribution, to name only a few [12-15]. Among the plethora of biomaterials and synthetic polymers explored as fundamental blocks for creating nanopharmaceuticals tailored for targeted drug delivery of a wide array of substances, ranging from small drugs and therapeutic proteins to nucleic acids and genes, particular attention is devoted to the protein-based nanosystems [13-15]. Their appeal lies in numerous advantageous attributes, such as: i) biocompatibility and biodegradability; ii) extraordinary binding capacity for various drugs; iii) abundance of proteins available from natural sources; iv) drug protection from enzymatic degradation and rapid renal excretion; v) gentle formulation and drug encapsulation requirements; vi) capability of surface covering with ligands specific to target tissues, vii) streamlined synthesis procedures with cost-effective outcomes [13-16]. Moreover, owing to the presence of numerous binding pockets and functional groups within the proteins, protein nanocarriers are especially promising for the development of effective multifunctional nanotheranostic systems merging both the therapeutic and diagnostic properties [17-19]. Theranostic nanomedicines assume the simultaneous integration of a therapeutic drug and visualizing agent for control of drug release, monitoring the changes at the target site in response to the treatment, and providing valuable insights into the effectiveness of the intervention at an early stage [17-18]. The fabrication of these advanced second-generation nanosystems requires a comprehensive understanding of the possible interactions within the complex systems.

In our previous work, we employed the multiple ligand simultaneous docking technique to investigate the interactions among four functionally significant proteins (cytochrome *c*, serum albumin, lysozyme and insulin), four antiviral drugs (favipiravir, molnupiravir, nirmatrelvir and ritonavir) and a series of cyanine dyes represented by four monomethines and two heptamethines. Our primer focus was to identify the most suitable systems for creating the protein nanoparticles carrying both antiviral drugs and cyanine dyes as visualizing agents [20]. The obtained results indicate that the albumin-based nanosystems functionalized by the heptamethine cyanine dyes can serve as effective carriers for targeted delivery of the explored antiviral agents. In continuation of our previous work, in the present study we extended our investigation to other cyanine dyes (six trimethines and seven pentamethines). The main was threefold: i) to delve

Cite as: O. Zhytniakivska, U. Tarabara, K. Vus, V. Trusova, G. Gorbenko, East Eur. J. Phys. 4, 318 (2023), https://doi.org/10.26565/2312-4334-2023-4-42

into the interactions within the ternary protein-dye-drug complexes using the multiple ligand simultaneous docking (MLSD) technique; ii) to identify the most promising candidates for the development of protein-based theranostic drug delivery nanoplatforms; iii) to determine the structural features of the cyanine dyes responsible for their loading in the multicomponent protein-based drug delivery nanosystems.

MATERIALS AND METHODS

Molecular docking studies

The three-dimensional X-ray crystal structures of the examined proteins in their native monomeric form were obtained from the Protein Data Bank using the PDB IDs 1REX, 3I40, 3ZCF, 6M4R for lysozyme (Lz), insulin (Ins), cytochrome *c* (Ct) and serum albumin (SA), respectively. The structural model for serum albumin was prepared by employing the DockPrep module of UCSF Chimera molecular software [21]. This involved the removal of water molecules and the addition of polar hydrogen atoms and Kollman charges [21]. The structure of the antiviral drugs (favipiravir, molnupiravir, nirmatrelvir and ritonavir) [20] and the investigated cyanine dyes (Figure 1) were constructed using the MarvinSketch (version 18.10.0) and optimized in Avogadro (version 1.1.0) using the Universal Force Field with the steepest descent algorithm [22,23]. Notably, counterions were omitted from the dye structures to retain molecular charges. Initially, the blind docking of the drugs or dyes (control dye-protein systems) with the proteins was carried out using the PatchDock server (http://bioinfo3d.cs.tau.ac.il/PatchDock/php.php) which focuses on finding the maximum surface shape complementarity while minimizing the steric clashes [24]. Subsequently, the top-scored docked drug-protein complexes were utilized as a receptor for docking of the second ligand, which represents either a trimethine or pentamethine cyanine dye, using the PatchDock server. To characterize the possible interactions involved in the formation of composite drug-dye-protein systems, the protein-ligand interaction profiler (PLIP, https://plip-tool.biotec.tudresden.de/plip-web/plip/index) was employed [25]. The selected docking poses were visualized using the UCSF Chimera software (version 1.14), combining the docking models with the best geometric shape complementarity in the same image to optimize visibility of the binding sites [26].

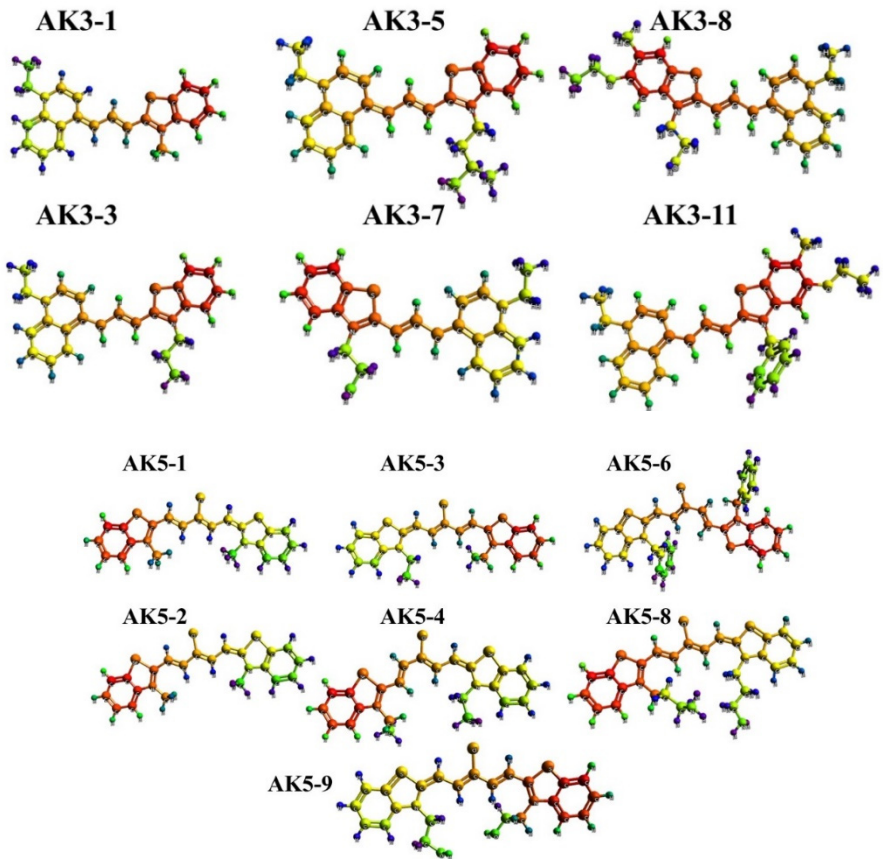

Figure 1. Structural formulas of the examined cyanine dyes

RESULTS AND DISCUSSION

The ternary complexes with the highest scores, comprising proteins, drugs, and dyes are depicted in Fig.2 (the drugs and dyes binding modes were identified for cytochrome *c* (Fig. 2), albumin (Fig. 3), lysozyme (Fig. 4) and insulin (Fig. 5). The examined tri- and pentamethines as well as previously reported mono- and heptamethines [20] are situated in close proximity to each other near the surfaces of cytochrome *c*, lysozyme and insulin. The binding sites for favipiravir,

molnupiravir, nirmatrelvir and ritonavir did not change compared to our previous findings [20]. However, the distinct binding pockets of albumin are observed for the drugs and the cyanine dyes examined here.

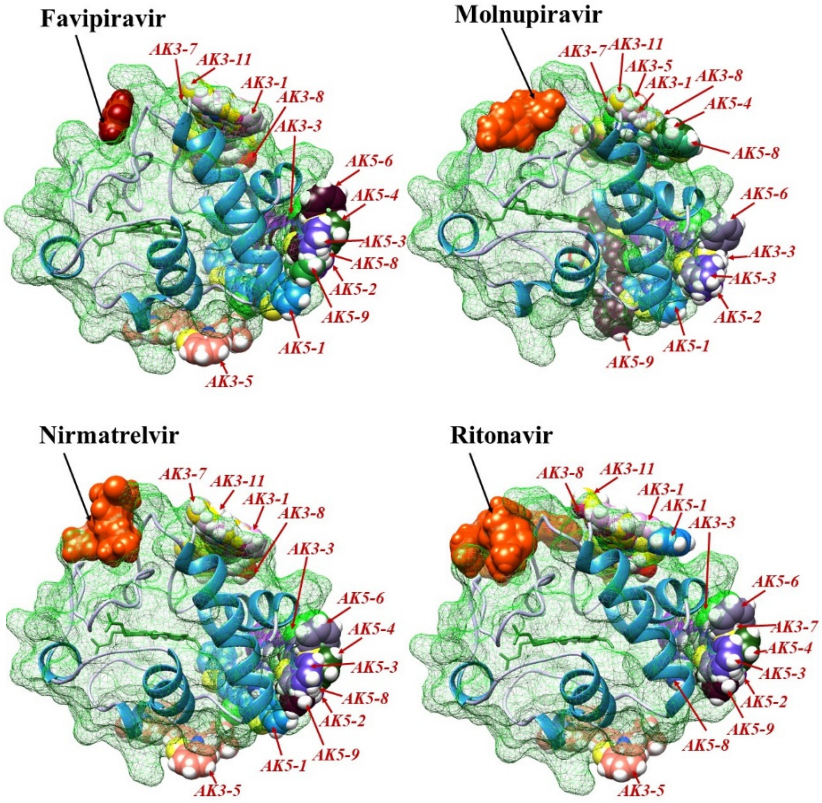

Figure 2. The highest-score docking poses obtained for cytochrome *c* using the MLSD in PatchDock

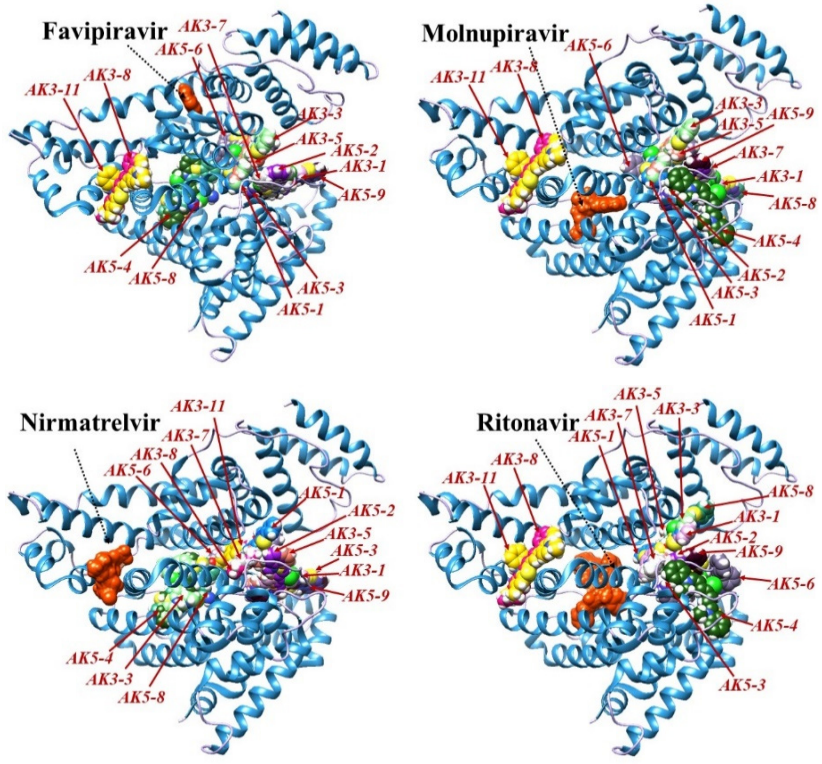

Figure 3. The highest-score docking poses obtained for albumin using the MLSD in PatchDock

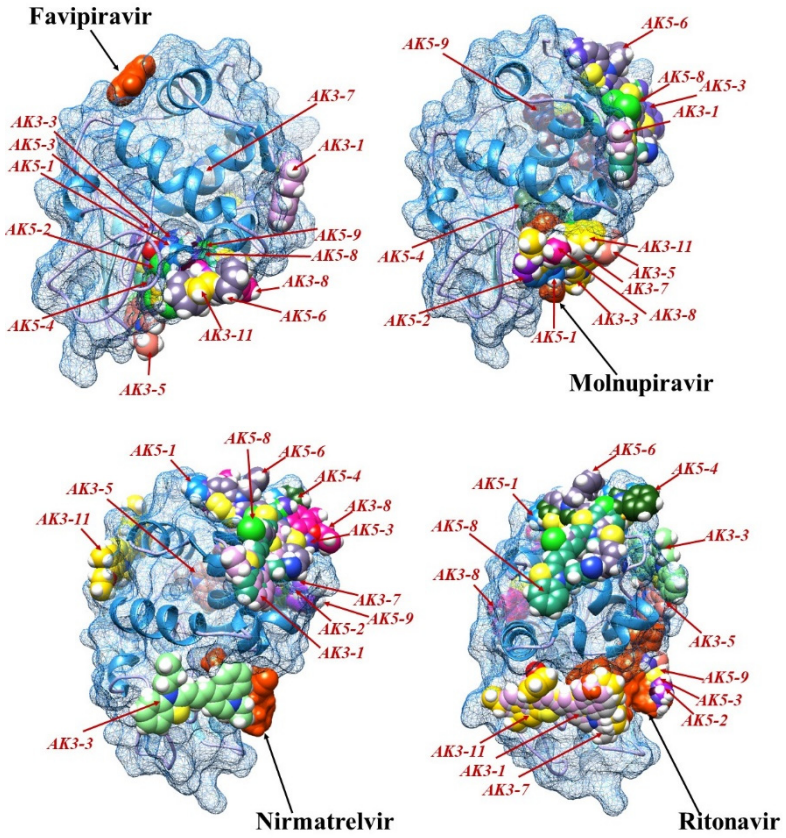

Figure 4. The highest-score docking poses obtained for lysozyme using the MLSD in PatchDock.

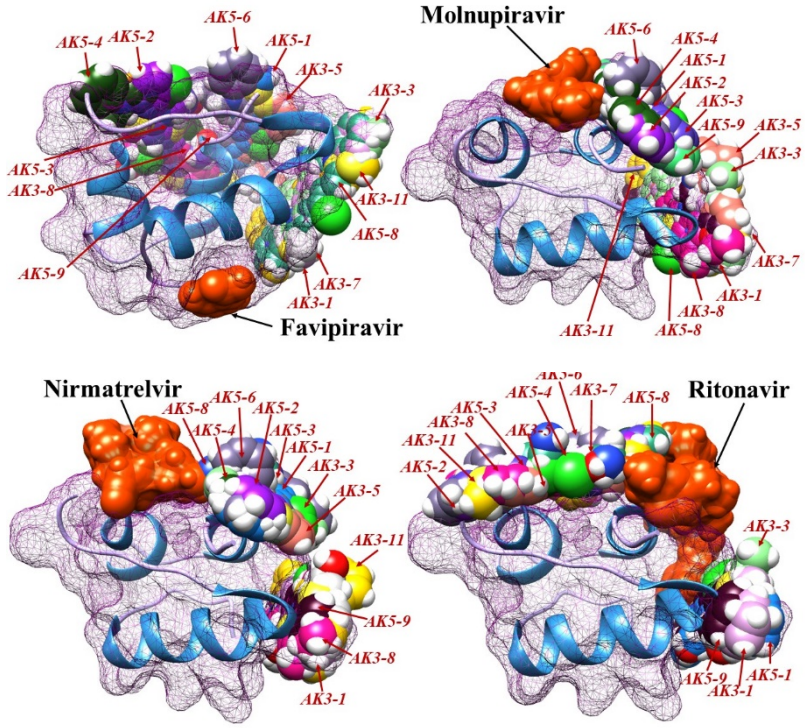

Figure 5. The highest-score docking poses obtained for insulin using the MLSD in PatchDock.

Next, the geometric shape complementarity scores and approximate interface areas for the protein-drug-dye systems were analyzed. In the cytochrome *c*-drug-dye systems the antiviral agents have no impact on the docking positions compared to the protein-dye complexes (Table 1). This observation does not hold true only in the specific cases of AK3-

3, AK3-5, (AK5-3), AK5-4, AK5-8, AK5-for molnupiravir and AK3-1, AK3-7, AK3-8, AK3-11, AK5-1 for ritonavir, where the dye-protein affinity slightly decrease (increase). The interface area slightly decreased (increased) by molnupiravir in the systems with AK3-3, AK3-5, (AK5-3), AK5-4, AK5-8, AK5-9 and increased by ritonavir for ternary complexes with the AK3-7, AK3-8, AK3-11, AK5-1. For the rest examined systems including previously reported [20], the comparison of the docking outcomes was performed in order to detect the most prospective dyes. It was found that the dye-protein affinity follows the order: AK7-5 > AK7-6 > AK5-6 > AK-1-2-20 > AK-1-2-19 > AK3-11 > AK5-8 (F, N, R) > AK5-9 (F, N, R) > AK3-5 (F, N, R) > AK3-8 > AK5-3 (F, N, R), AK3-3 (F, N, R) > AK3-7 (F, M, N) > AK5-2 > AK5-4 (F, N, R)> AK-1-2-17 > AK5-1 > AK3-1 > AK-1-2-18; while the interface area decreases in the order: AK7-6 > AK7-5 > AK5-6 > AK-1-2-20 > AK-1-2-19 > AK5-8 > AK5-9 > AK3-3 > AK3-11 > AK5-3 > AK-1-2-17 > AK3-5 > AK-1-2-18 > AK5-2 > AK5-4 > AK3-8 > AK5-1 > AK3-7 > AK3-1.

Table 1. The geometric shape complementarity score and approximate interface area of the complex derived for the cytochrome *c*-drug-dye systems (F- Favipiravir, M – Molnupiravir, N - Nirmatrelvir, R – Ritonavir).

Cytochrome *c*										
Dye	**Score**					**Approximate interface area of the complex, A^2**				
	F	**M**	**N**	**R**	**-**	**F**	**M**	**N**	**R**	**-**
-	2220	3648	4292	6062	-	237.40	384.30	576.30	797.80	-
AK3-1	4578	4578	4578	4636	4578	500.30	500.30	500.30	506.60	500.30
AK3-3	4944	4788	4944	4944	4944	616.00	593.80	616.00	616.00	616.00
AK3-5	5062	4962	5062	5062	5062	600.90	583.90	600.90	600.90	600.90
AK3-7	4780	4780	4780	4678	4780	522.80	522.80	522.80	600.80	522.80
AK3-8	5034	5034	5034	5016	5034	561.70	561.70	561.70	572.90	561.70
AK3-11	5372	5372	5372	5440	5372	614.20	614.20	614.20	647.90	614.20
AK5-1	4584	4584	4584	4666	4584	527.10	527.10	527.10	531.90	527.10
AK5-2	4736	4736	4736	4736	4736	579.10	579.10	579.10	579.10	579.10
AK5-3	4944	5200	4944	4944	4944	610.90	627.30	610.90	610.90	610.90
AK5-4	4734	4604	4734	4734	4734	563.30	582.80	563.30	563.30	563.30
AK5-6	5638	5638	5638	5638	5638	766.10	766.10	766.10	766.10	766.10
AK5-8	5266	4970	5266	5266	5266	675.10	632.70	675.10	675.10	675.10
AK5-9	5122	4932	5122	5122	5122	632.00	584.70	632.00	632.00	632.00

The drug influence on the docking parameters in the albumin-cyanine systems was found to be more pronounced (Table 2). The docking score remains the same for the systems AK3-1 + F/M/N, AK3-3 + N, AK3-5 + N, AK3-7 + N, AK3-8 + F/M/R, AK3-11 + F/M/R, AK5-1 + N, AK5-2 + N, AK5-3 + all drug systems, AK5-4 + F/N, AK5-6 + F/M/N, AK5-8 + F/N, AK5-9 + F/N; decreases in the systems AK3-5 + F/M/R, AK3-7 + F/M/R, AK3-8 + N, AK3-11 + N, AK5-1 + F/M, AK5-2 + F/M, AK5-8 + M/R, AK5-9 + M/R; and increases in the systems AK3-1+R, AK3-3 + F/M/R, AK5-1+ R, AK5-2 + R, AK5-4 + M/R, AK5-6 +R. The ranking of the explored complexes according to aforementioned parameter appeared to be as follows: AK7-5 (N) > AK7-6 > AK-1-2-20 (F, M, N) > AK-1-2-19 (N) > AK3-11 (F, M, R) > AK5-8 (F, N, R) > AK5-6 (F, M, N) > AK-1-2-18 (F, N) > AK-1-2-17 (F, N) > AK5-9 (F, N) > AK3-8 (F, M, R) > AK3-5 (N) > AK5-4 (F, N)> AK5-3 > AK3-3 (N) > AK5-1 (N) > AK3-7 (N) > AK3-1 (F, M, N) > AK5-2 (N). The highest albumin-cyanine interface area was observed for AK7-5 (N, R), AK-1-2-20 (F, M, N), AK7-6, AK-1-2-19, AK5-6, AK5-8, AK3-11.

Table 2. The geometric shape complementarity score and approximate interface area of the complex derived for the albumin-drug-dye systems (F- Favipiravir, M – Molnupiravir, N - Nirmatrelvir, R – Ritonavir)

Serum albumin										
Dye	**Score**					**Approximate interface area of the complex, A^2**				
	F	**M**	**N**	**R**	**-**	**F**	**M**	**N**	**R**	**-**
-	2900	5054	6212	8412	-	343.60	553.10	719.50	1036.60	-
AK3-1	5280	5280	5280	5332	5280	600.50	600.50	600.50	626.60	600.50
AK3-3	5672	5672	5606	5672	5606	677.80	677.80	672.80	677.80	672.80
AK3-5	5824	5824	6030	5792	6030	739.20	739.20	690.50	746.80	690.50
AK3-7	5306	5306	5372	5320	5372	636.90	636.90	658.80	690.30	658.80
AK3-8	6074	6074	6022	6074	6074	695.60	695.60	730.90	695.60	695.60
AK3-11	6634	6634	6428	6634	6634	753.10	753.10	834.70	753.10	753.10
AK5-1	5338	5338	5406	5560	5406	682.90	682.90	672.80	674.40	672.80
AK5-2	5198	5198	5208	5234	5208	634.70	634.70	639.00	647.20	639.00
AK5-3	5854	5854	5854	5854	5854	683.60	683.60	683.60	683.60	683.60
AK5-4	5868	5870	5868	5870	5868	681.40	747.80	681.40	747.80	681.40
AK5-6	6556	6556	6556	6960	6556	814.60	814.60	814.60	914.90	814.60
AK5-8	6562	5922	6562	5944	6562	775.70	695.90	775.70	690.00	775.70
AK5-9	6188	5948	6188	5948	6188	691.90	700.10	691.90	700.10	691.90

Table 3. The geometric shape complementarity score and approximate interface area of the complex derived for the lysozyme-drug-dye systems (F- Favipiravir, M – Molnupiravir, N - Nirmatrelvir, R – Ritonavir).

Lysozyme										
Dye	Score					Approximate interface area of the complex, A^2				
	F	**M**	**N**	**R**	**-**	**F**	**M**	**N**	**R**	**-**
-	2184	3628	4690	5922	-	245.40	394.70	522.30	702.70	-
AK3-1	4212	4212	4212	4232	4212	481.80	481.80	481.80	530.10	481.80
AK3-3	4520	4646	4514	4538	4520	507.50	540.90	538.10	574.80	507.50
AK3-5	4634	4708	4606	4600	4634	548.40	557.60	493.70	605.30	548.40
AK3-7	4334	4344	4334	4462	4334	537.20	525.50	537.20	547.80	537.20
AK3-8	4872	4866	4718	4706	4872	580.60	570.50	489.30	604.30	580.60
AK3-11	5176	5198	5044	5228	5176	626.40	641.60	604.80	671.30	626.40
AK5-1	4526	4680	4502	4546	4526	510.70	554.40	584.20	569.20	510.70
AK5-2	4534	4656	4382	4428	4534	522.40	547.50	556.40	549.30	522.40
AK5-3	4812	4548	4548	4702	4812	544.30	517.40	517.40	572.10	544.30
AK5-4	4624	4580	4522	4624	4624	531.50	506.00	662.40	545.50	531.50
AK5-6	5550	5304	5304	5218	5550	652.70	614.70	614.70	628.20	652.70
AK5-8	5196	4992	4992	4992	5196	585.10	556.80	556.80	556.80	585.10
AK5-9	5004	4640	4640	4680	5004	547.40	589.50	589.50	569.10	547.40

Table 4. The geometric shape complementarity score and approximate interface area of the complex derived for the insulin-drug-dye systems (F- Favipiravir, M – Molnupiravir, N - Nirmatrelvir, R – Ritonavir).

Insulin										
Dye	Score					Approximate interface area of the complex, A^2				
	F	**M**	**N**	**R**	**-**	**F**	**M**	**N**	**R**	**-**
-	1944	2826	3544	4582	-	244.40	327.80	410.40	619.30	-
AK3-1	4096	4096	4096	3848	4096	460.40	460.40	460.40	436.70	460.40
AK3-3	4202	4202	4366	4112	4202	469.30	469.30	493.60	472.90	469.30
AK3-5	4234	4070	4208	4386	4234	476.80	457.50	480.00	564.40	476.80
AK3-7	4046	4046	4046	4072	4046	447.50	447.50	447.50	505.10	447.50
AK3-8	4560	4456	4456	4568	4560	572.40	547.80	547.80	561.20	572.40
AK3-11	4536	4536	4536	5044	4536	534.00	534.00	534.00	646.50	534.00
AK5-1	4268	4202	4154	3946	4268	477.40	477.30	477.80	458.00	477.40
AK5-2	4276	4010	3984	3980	4276	529.20	474.70	471.40	506.50	529.20
AK5-3	4298	4086	4094	4320	4298	556.80	476.50	480.60	513.90	556.80
AK5-4	4242	4300	4268	4388	4242	552.50	508.30	528.00	527.20	552.50
AK5-6	4560	4844	4792	4584	4560	532.70	564.90	555.00	602.00	532.70
AK5-8	4392	4392	4428	4330	4392	523.60	523.60	528.80	533.00	523.60
AK5-9	4392	4366	4342	4172	4392	551.00	541.80	516.20	509.60	551.00

The docking score remains the same for all lysozyme-favipiravir-dye complexes (Table 3) and for the systems: AK3-1 + M/N, AK3-7 + N, AK5-4 + R; decreases in the systems: AK3-3 + N, AK3-5 + N/R, AK3-8 + M/N/R, AK3-11 + N, AK5-1 +N, AK5-2 + N/R, AK5-3 + M/N/R, AK5-4 + M/N, AK5-6 + M/N/R, AK5-8 + M/N/R, AK5-9 + M/N/R; and increases in the systems: AK3-1 + R, AK3-3 + M/R, AK3-5 + M, AK3-7 + M/R, AK3-11 + M/R, AK5-1 + M/R, AK5-2 + M. The dye-lysozyme affinity was found to follow the order: AK7-5 > AK-1-2-20 > AK7-6 > AK5-6 > AK-1-2-19 > AK-1-2-18 > AK5-8> AK3-11 > AK5-9 > AK-1-2-17 > AK3-8 > AK5-3 > AK3-5 > AK5-4> AK5-2 > AK5-1 > AK3-3 > AK3-7 > AK3-1, while the highest protein-cyanine interface area was observed in the case of AK-1-2-20, AK7-5, AK-1-2-19, AK7-6, AK5-6, AK3-11. The favipiravir do not exert influence on the dye-protein affinity and interface area in the cases of insulin and lysozyme (Table 4). The score remains the same for the complexes: AK3-1 + M/N, AK3-3 + M, AK3-7 + M/N, AK3-11 + M/N; decreases in the systems: AK3-1 + R, AK3-3 + R, AK3-5 + M/N, AK3-8 + M/N, AK5-1 +M/N/R, AK5-2 +M/N/R, AK-3 +M/N, AK5-8 + R, AK5-9 + M/N/R; and increases in the systems: AK3-3 + N, AK3-5 + R, AK3-7 + R, AK3-8 + R, AK3-11 + R, AK5-3 + R, AK5-4 +M/N/R, AK5-6 +M/N/R, AK5-8 + N. The dye-insulin affinity decreases in the order: AK-1-2-19 > AK-1-2-20 > AK7-6 > AK7-5 > AK5-6, AK3-8 > AK3-11 > AK5-8, AK5-9 > AK5-3 > AK5-2 > AK5-1 > AK5-4> AK3-5 > AK3-3, AK-1-2-18 > AK3-1 > AK3-7 > AK-1-2-17, while the interface area follows the order: AK-1-2-19 > AK7-6 > AK-1-2-20 > AK7-5 > AK3-8 > AK5-3 > AK5-4 > AK5-9 > AK3-11 > AK5-6 > AK5-2 > AK5-8 > AK5-1 > AK3-5 > AK-1-2-18 > AK3-3 > AK3-1 > AK3-7 > AK-1-2-17. The crucial contribution of hydrophobic interactions in all examined dye-protein complexes was revealed by the PLIP analysis. The other types of interactions involved hydrogen bonds, salt and water bridges.

CONCLUSIONS

In conclusion, the present study was focused on the use of multiple ligand simultaneous docking technique to investigate the interactions between the four functionally significant proteins (cytochrome c, serum albumin, lysozyme

and insulin), four antiviral drugs (favipiravir, molnupiravir, nirmatrelvir and ritonavir) and the cyanine dyes (six trimethines and seven pentamethines). The comparison with ternary complexes from our previous work (that included four monomethines and two heptamethines) was conducted. The obtained results indicate that the dye-protein affinity seems to be not directly dependent on the polymethine chain length. The strongest complexes with the proteins were formed by the heptamethines (AK7-5, AK7-6), monomethines with CH_3O substitution (AK-1-2-20, AK-1-2-19), pentamethines with $CH_2C_6H_6$ and C_3H_4N substitution (AK5-6, AK5-8), trimethines with OC_2H_5 and CH_3 substitution (AK3-11, AK3-8). Among the examined proteins, the cyanine dyes showed the highest affinity binding to the albumin molecule, while the lowest values of the docking score were observed for insulin. The other results include: i) the cyanines and drugs occupy the different binding sites, except the lysozyme cavity that seems to be suitable for accommodation of both ligands (in the case of molnupiravir, nirmatrelvir and ritonavir); ii) the obtained complexes are predominantly stabilized by hydrophobic forces.

Overall, the most prospective drug delivery systems with the trimethines and pentamethines as visualizing agents are AK5-6-, AK5-8- and AK3-11-drug-albumin complexes, but, generally, the albumin-based nanosystems functionalized by the heptamethine cyanine dyes seem to be the most effective carriers for targeted delivery of the explored antiviral agents.

Acknowledgements

This work was supported by the Ministry of Education and Science of Ukraine (the project "Development of novel means of medical diagnostics by biomedical nanotechnologies and modern ultrasonic and fluorescence methods").

ORCID IDs

Olga Zhytniakivska, https://orcid.org/0000-0002-2068-5823; **Uliana Tarabara,** https://orcid.org/0000-0002-7677-0779
Kateryna Vus, https://orcid.org/0000-0003-4738-4016; **Valeriya Trusova,** https://orcid.org/0000-0002-7087-071X
Galyna Gorbenko, https://orcid.org/0000-0002-0954-5053

REFERENCES

[1] Md. I. Khan, M.I. Hossain, M.K. Hossain, M.H.K. Rubel, K.M. Hossain, et al., ACS. Appl. Bio Mater. 5, 971 (2022). https://doi.org/10.1021/acsabm.2c00002
[2] J. Wang, Y. Li, and G. Nie, Nat. Rev. Mat. **6**, 766 (2021). https://doi.org/10.1038/s41578-021-00315-x
[3] X. Sun, J. Wang, Z. Wang, C. Zhu, J. Xi, L. Fan, J. Han, and R. Guo, J. Colloid Interface Sci. **610**, 89 (2022). https://doi.org/10.1016/j.jcis.2021.11.189
[4] E. Nance, S.H. Pun, R. Saigal, and D.L. Sellers, **7**, 31 (2022). https://doi.org/10.1038/s41578-021-00394-w
[5] T.P. Crowe, and W.H. Hsu, Pharmaceutics, **14**, 629 (2022). https://doi.org/10.3390/pharmaceutics14030629
[6] A.S. Ali, M.G. Alrashedi, O.A.A. Ahmed, I.M. Ibrahim, Polymers, **14**, 2616 (2022). https://doi.org/10.3390/polym14132616
[7] N.B. Kiremitler, M.Z. Kemerli, and N. KAyaci, et al., ACS Appl. Nano Mater. **5**, 6029 (2022). https://doi.org/10.1021/acsanm.2c00181
[8] C. Medina-Montano, I. R. Berti, R. C. Gambaro, M.J. Limeres, M. Svensson, et al., Pharmaceutics, **14**, 1611 (2022). https://doi.org/10.3390/pharmaceutics14081611
[9] M. Ferreira, L.L. Chaves, S.A. Costa Lima, S. Reis, Int. J. Pharm. **492**, 65 (2015). https://doi.org/10.1016/j.ijpharm.2015.07.013
[10] Y. Deng, X. Zhang, H. Shen, Q. He, Z. Wu, W. Liao, and M. Yuan, Front. Bioeng. Biotechnol. **7**, (2019). https://doi.org/10.3389/fbioe.2019.00489
[11] T. Alam, M.A. Ansari, S. Baboota, and J. Ali, Drug Deliv. Transl. Res. **12**, 577 (2022). https://doi.org/10.1007/s13346-021-00958-x
[12] H. Zhang, T. Fan, W. Chen, Y. Li, and B. Wang, Bioactive Materials. **5**, 1071 (2020). https://doi.org/10.1016/j.bioactmat.2020.06.012
[13] A.L. Martínez-López, C. Pangua, C. Reboredo, R. Campión, J. Morales-Gracia, and J.M. Irache, Int. J. Pharm. **581**, 119289 (2020). https://doi.org/10.1016/j.ijpharm.2020.119289
[14] A.O. Elzoghby, W.M. Samy, and N.A. Elgindy, Journal of Controlled Release, **161**, 38 (2012). https://doi.org/10.1016/j.jconrel.2012.04.036
[15] E. Kianfar, J. Nanobiotechnol. **19**, 159 (2021). https://doi.org/10.1186/s12951-021-00896-3
[16] C. Wen, J. Zhang, H. Zhang, Y. Duan, Foods. **11**, 1701 (2022). https://doi.org/10.3390/foods11121701
[17] S. Lee, T.C. Pham, C. Bae, Y. Choi, Y.K. Kim, and J. Yoon, Coord. Chem. Rev. **412**, 213258 (2020). https://doi.org/10.1016/j.ccr.2020.213258
[18] L. Xu, S.-B. Wang, C. Xu, D. Han, X.-H. Ren, X.-Z. Zhang, and S.-X. Cheng, ACS Appl. Mater. Interfaces. **11**, 38385 (2019). https://doi.org/10.1021/acsami.9b11263
[19] Y. Wang, H. Igbal, U. U.-Rehman, L. Zhai, Z. Yuan, A. Razzaq, M. Lv, et al., J. Drug Deliv. Sci. Technol. **79**, 104072 (2023). https://doi.org/10.1016/j.jddst.2022.104072
[20] O. Zhytniakivska, U.K. Vus, V. Trusova, and G. Gorbenko, East. European Journal of Physics, **3**, 585 (2023). https://doi.org/10.26565/2312-4334-2023-3-69
[21] E. Pettersen, T. Goddard, C. Huang, G. Couch, D. Greenblatt, E. Meng, and T. Ferrin, UCSF Chimera – a visualization system for exploratory research and analysis, J. Comput. Chem. **25**, 1605–1612(2004). https://doi.org/10.1002/jcc.20084
[22] P. Csizmadia, in: *Proceedings of ECSOC-3, the third international electronic conference on synthetic organic chemistry*, (1999), pp. 367-369. https://doi.org/10.3390/ECSOC-3-01775
[23] M.D. Hanwell, D.E. Curtis, D.C. Lonie, T. Vandermeersch, E. Zurek, and G.R. Hutchison, J. Cheminform. **4**, 17 (2012). https://doi.org/10.1186/1758-2946-4-17
[24] D. Schneidman-Duhovny, Y. Inbar, R. Nussinov, and H.J. Wolfson, Nucl. Acids. Res. **33**, W363 (2005). https://doi.org/10.1093/nar/gki481

[25] M.F. Adasme, K.L. Linnemann, S.N. Bolz, F. Kaiser, S. Salentin, V.J. Haupt, and M. Schroeder, Nucl. Acids. Res. **49**, W530 (2021). https://doi.org/10.1093/nar/gkab294
[26] E.F. Pettersen, T.D. Goddard, C.C. Huang, G.S. Couch, D.M. Greenblatt, E.C. Meng, and T.E. Ferrin, J. Comput. Chem. **25**, 1605 (2004). https://doi.org/10.1002/jcc.20084

ОДНОЧАСНИЙ ДОКІНГ ПРОТИВІРУСНИХ ПРЕПАРАТІВ ТА ЦІАНІНОВИХ БАРВНИКІВ З БІЛКАМИ З ВИКОРИСТАННЯМ МУЛЬТИЛІГАНДНОГО ПІДХОДУ

Ольга Житняківська, Уляна Тарабара, Катерина Вус, Валерія Трусова, Галина Горбенко

Кафедра медичної фізики та біомедичних нанотехнологій, Харківський національний університет імені В.Н. Каразіна м. Свободи 4, Харків, 61022, Україна

Наносистеми на основі білків для цільової доставки широкого спектру лікарських засобів, починаючи від невеликих ліків і терапевтичних білків до нуклеїнових кислот і генів, привертають все більшу увагу завдяки своїй біосумісності та здатності до біодеградації, надзвичайній здатності до зв'язування різних лігандів, доступності з природних джерел, ефективному захисту ліків і м'яким умовам інкапсуляції тощо. Завдяки численним центрам зв'язування та функціональним групам на поверхні білків, ці наноносії є високоефективними багатофункціональними нанотераностичними системами, які можуть включати як терапевтичний препарат, так і візуалізуючий агент. Ця інтеграція служить багатьом цілям, включаючи регулювання вивільнення ліків, моніторинг змін у цільовій ділянці у відповідь на лікування та оцінку ефективності втручання на ранніх стадіях. Розробка цих передових наносистем другого покоління вимагає детального розуміння потенційних взаємодій у цих складних системах. У даній роботі ми оцінили потенціал шести триметинових та семи пентаметинових ціанінових барвників як потенційних візуалізуючих агентів в системах білок-лікарський препарат, що включали функціонально важливі білки (цитохром *c*, сироватковий альбумін, лізоцим та інсулін) та чотири противірусних препарати (фавіпіравір, молнупіравір, нірматрелвір і ритонавір). Для всіх груп досліджуваних ціанінових барвників визначені потрійні системи з найвищою комплементарністю форми поверхні барвник-білок, а також типи стабілізуючих взаємодій. Проведено оцінку впливу структури ціанінових барвників на стабільність комплексів лікарський препарат-білок-зонд. Отримані результати вказують на те, що спорідненість барвник-білок не залежить безпосередньо від довжини поліметинового ланцюга. Виявлено, що найбільш перспективними системами доставки ліків, що містять розглянуті триметини та пентаметини як візуалізуючі агенти, це комплекси АК5-6-, АК5-8- та АК3-11-ліки-альбумін.

Ключові слова: *комплекси білок-лікарський препарат-барвник; противірусні агенти; білкові наночастинки; наноносії ліків; ціанінові барвники; одночасний молекулярний докінг*